Journal of Anatomy

J. Anat. (2014) **224**, pp647–658 doi: 10.1111/joa.12177

Microstructural changes in cartilage and bone related to repetitive overloading in an equine athlete model

Sean M. Turley,[1] Ashvin Thambyah,[1] Christopher M. Riggs,[2] Elwyn C. Firth[3] and Neil D. Broom[1]

[1]*Tissue Mechanics Laboratory, Department of Chemical and Materials Engineering, University of Auckland, Auckland, New Zealand*
[2]*Department of Veterinary Clinical Services, Hong Kong Jockey Club, Sha Tin Racecourse, Hong Kong, China*
[3]*Department of Sport and Exercise Science, Faculty of Science, University of Auckland, Auckland, New Zealand*

Abstract

The palmar aspect of the third metacarpal (MC3) condyle of equine athletes is known to be subjected to repetitive overloading that can lead to the accumulation of joint tissue damage, degeneration, and stress fractures, some of which result in catastrophic failure. However, there is still a need to understand at a detailed microstructural level how this damage progresses in the context of the wider joint tissue complex, i.e. the articular surface, the hyaline and calcified cartilage, and the subchondral bone. MC3 bones from non-fractured joints were obtained from the right forelimbs of 16 Thoroughbred racehorses varying in age between 3 and 8 years, with documented histories of active race training. Detailed microstructural analysis of two clinically important sites, the parasagittal grooves and the mid-condylar regions, identified extensive levels of microdamage in the calcified cartilage and subchondral bone concealed beneath outwardly intact hyaline cartilage. The study shows a progression in microdamage severity, commencing with mild hard-tissue microcracking in younger animals and escalating to severe subchondral bone collapse and lesion formation in the hyaline cartilage with increasing age and thus athletic activity. The presence of a clearly distinguishable fibrous tissue layer at the articular surface immediately above sites of severe subchondral collapse suggested a limited reparative response in the hyaline cartilage.

Key words: calcified cartilage; equine athlete; hyaline cartilage; MC3; microdamage; overload arthrosis; repair; subchondral bone.

Introduction

Excessive mechanical loading such as repetitive impact is known to lead to the formation of microcracks in both the subchondral bone (Radin et al., 1973; Zioupos & Currey, 1994; Martin et al., 1996) and calcified cartilage (Mori et al., 1993; Sokoloff, 1993). With continued loading, crack density increases if the remodelling response is unable to keep pace with the rate of new crack formation (Schaffler et al., 1989; Mori et al., 1993; Martin et al., 1996). High levels of microdamage, interacting with the complex biological responses of the osteochondral tissues, can lead to the formation of much larger scale 'stress' fractures (Riggs, 2002) or to degeneration and ultimate loss of the overlying articular cartilage (Burr & Radin, 2003).

Correspondence
Neil D. Broom, Department of Chemical and Materials Engineering, University of Auckland, Private Bag 92019, Auckland Mail Centre, Auckland 1142, New Zealand. E: nd.broom@auckland.ac.nz

Accepted for publication *25 February 2014*
Article published online *1 April 2014*

The palmar aspect of the third metacarpal condyle (MC3) of the Thoroughbred racehorse is a region subjected to intense repetitive loading and high bone strains (Biewener, 1993), conditions which can lead to an accumulation of microdamage and eventually to a loss of joint health. One manifestation of microdamage-induced pathology in this region is known as palmar osteochondral disease (POD), which is believed to result from the repetitive cyclical overextension of the metacarpophalangeal joint associated with high intensity exercise (Pool, 1996; Norrdin et al., 1998; Barr et al., 2009). This condition, which also occurs in the similar metatarsophalangeal joint of the equine hindlimb, may be classified as a form of 'overload arthrosis', with similar conditions also found in human athletes and joggers, and in those affected by obesity or joint malalignment (Frost, 1994).

Osteochondral disease lesions appear as focal sites of subchondral bone failure and occur at consistent locations on either the lateral or medial condyles (Pool, 1996), in a well-defined region of the joint known to experience very high *in vivo* loading during high speed locomotion (Biewener et al., 1983; Harrison et al., 2010). The earliest sign of POD is 'bruising' of the subchondral bone, resulting in

discoloration that is visible through the still intact hyaline cartilage. Later stages of the disease involve subchondral bone disruption accompanied by varying levels of cartilage degeneration, leading ultimately to subchondral bone collapse and ulceration of the cartilage (Riggs, 2006).

Although common among athletically trained horses, with a reported prevalence of 80% (Pinchbeck et al., 2013b), the pathological changes associated with POD are difficult to detect clinically. It is physically impossible to view the POD lesion sites during routine arthroscopic examination (Riggs, 2006) and only severe lesions are readily detectable on routine radiography (Richardson, 2003). As a consequence, the lesions often remain undiagnosed until the late stages of disease, at which point the pathological changes are irreversible, resulting in chronic joint disease (Barr et al., 2009).

The parasagittal grooves of the palmar MC3 are also affected by microdamage accumulation due to excessive loading. A common condition, known as a parasagittal linear defect, can be found in the parasagittal grooves of approximately 75% of training and racing Thoroughbreds in the UK (Riggs et al., 1999). These defects are characterised by linearly aligned cracks in the calcified cartilage (Riggs et al., 1999) and subchondral bone (Riggs et al., 1999; Radtke et al., 2003), and are associated with bone sclerosis induced by the cyclic loading experienced during training and racing (Reilly et al., 1997). These changes precede the formation of catastrophic fractures at this site (Radtke et al., 2003) and it has been suggested that these fractures are the result of a fatigue process leading to the growth of a single dominant crack from within the array of microdamage (Radtke et al., 2003). This larger scale parasagittal 'condylar' fracture is common during racing and training (Ellis, 1994; Johnson et al., 1994) and is reported to account for approximately 25% of all catastrophic injuries among racing Thoroughbreds in California (Johnson et al., 1994). In fact, this type of fracture is one of the most frequent reasons for euthanasia among horses that sustain injuries while racing (Rick et al., 1983; Stephens et al., 1988).

Previous structural studies of damage accumulation in the palmar aspect of the equine MC3 can be broadly divided into three somewhat distinct categories: (i) gross examination (Radtke et al., 2003; Barr et al., 2009); (ii) focused microscopic assessment of specific structural features (Norrdin & Stover, 2006; Boyde et al., 2011); (iii) multi-scalar structural assessment (Norrdin et al., 1998; Muir et al., 2008). With respect to the substantial body of research noted above, there is still a need to understand at a detailed structural level how overload arthrosis progresses at this site and in the context of the functionally integrated joint tissue complex (i.e. the articular surface, the hyaline and calcified cartilage and the subchondral bone).

The consistent occurrence of microdamage at the distal end of the equine MC3 makes it a valuable model for understanding structural changes in the subchondral bone and overlying cartilage associated with excessive mechanical loading. The aim of this new study was to provide a broad microstructural survey of the effects of microdamage accumulation in the palmar aspect of the equine MC3 condyles occurring in the hyaline and calcified cartilage, and the subchondral bone, and to map the progression of disease through the presentation of a broad range of pathological states.

Methods

The right MC3 bone (Fig. 1A) was collected from 16 Thoroughbred racehorses that required euthanasia at the Hong Kong Jockey Club over a period of 6 months in 2008–2009. All horses were euthanised for reasons unrelated to the right metacarpophalangeal joint, and all but two animals (Horses 9 and 15) were in active race training within 4 weeks of being euthanised. The ages of the animals ranged between 3 and 8 years, and their number of race starts ranged from 2 to 57 (see Table 1).

Four animals were diagnosed clinically with osteoarthritis of the fetlock (Horses 7, 13, 14, and 16), one of which was diagnosed following surgery to address an osteochondral chip fracture (Horse 13). Six animals had reported histories of joint inflammation (Horses 7, 9, 12, 13, 14, and 15). Clinical data also indicated injury to the non-sampled left forelimb in a number of animals: one animal suffered a catastrophic fracture of the MC3 several centimetres proximal to the joint surface (Horse 10), and two animals suffered basilar fracture of the medial proximal sesamoid bone (Horses 4 and 7).

The MC3 bones, having been stored frozen below −20 °C, were defrosted in cold running water. The articular condyles were examined for gross defects using India ink staining to detect cartilage disruption, and then graded using an equine fetlock-specific macroscopic scoring system (Barr et al., 2009), of which two specific features were of particular relevance to the regions of interest presented in this study. The first feature, palmar osteochondral disease, was scored on a scale of zero (no evidence of POD) to three (established POD lesions with discoloration and disruption/collapse of the articular surface). The second feature of interest, linear fissures within the parasagittal grooves, is scored on a scale of zero

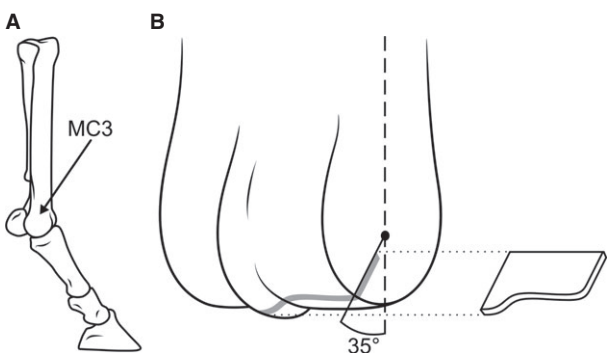

Fig. 1 Schematics demonstrating sampling location. (A) Schematic showing the MC3 in context of the distal equine forelimb. (B) Schematic of the distal end of MC3 indicating the region of interest in the palmar aspect, the black dot in the centre representing an approximation of the centre of rotation of the distal MC3. Exploded section approximates an osteochondral slab from which sections were taken for microscopic.

Table 1 A summary of history, microdamage, and macroscopic appearance in the mid-condylar region and parasagittal groove of the lateral (L) and medial (M) condyles for each horse. Younger and older animals are separated by a dotted line.

			Microdamage				Macroscopic appearance			
			Mid-condylar region		Parasagittal groove		POD		Linear fissures	
Horse	Age	Race starts	L	M	L	M	L	M	L	M
1	3	2	None	None	Moderate	Mild	0	0	1	1
2	3	7	None	None	Moderate	Mild	0	0	2	2
3	4	3	None	None	None	Mild	0	0	0	0
4	4	5	None	Moderate	Mild	Mild	0	2	1	1
5	4	6	None	Moderate	Mild	Moderate	0	0	1	1
6	4	6	None	None	Mild	Moderate	0	0	1	1
7	4	9	Mild	Moderate	Mild	Mild	1	1	0	1
8	5	8	None	None	Mild	Mild	0	1	0	1
9	5	8	None	None	Moderate	Mild	0	0	1	2
10	5	12	None	None	Mild	Mild	0	0	0	0
11	6	21	Moderate	Moderate	Moderate	Moderate	1	1	1	1
12	6	27	Moderate	Moderate	Mild	Mild	1	1	0	0
13	7	27	Moderate	Severe	Severe	Severe	2	3	1	2
14	7	50	Severe	Severe	Moderate	Moderate	2	2	1	1
15	8	56	Severe	Severe	Severe	Moderate	2	2	1	1
16	8	57	Mild	Mild	Mild	Mild	1	1	1	0

(no evidence of linear fissures) to three (well defined groove with full-thickness split in the cartilage). The grading was performed by one of the researchers (S.M.T.) as each bone was processed, with photographic images being used to ensure consistency of assessment once all MC3 bones had been analysed.

Osteochondral slabs in the mediolateral plane, ≈4 mm thick, were sawn from both the lateral and medial condyles of the palmar aspect. These slabs were aligned perpendicular to the joint surface, and inclined at ≈35° to the line of the centre of the bone shaft, such that they passed through the centre of rotation of the distal MC3 (Fig. 1B). This site was selected because of its association with commonly formed lesions (Pool, 1996) and the presumed highest *in vivo* loads (Firth et al., 2005), i.e. the contact site between the sesamoid bones and MC3 during the loading phase of high-speed locomotion (Stashak & Hill, 2002).

Each osteochondral slab was fixed in 10% formalin for 1 week, and then mildly decalcified in 10% formic acid for ≈10 days. Relatively thick (≈30 μm) osteochondral sections were obtained by cryosectioning. These sections were viewed in a fully hydrated state using transmission bright field microscopy and differential interference contrast (DIC) microscopy. Following the collection of full cross-sectional micrographs from all the animals, one of the researchers (S.M.T.) devised and implemented a microdamage grading system (Table 2) to categorise the extent of microdamage visible in each of the two regions of interest: the parasagittal groove and the mid-condylar region (Fig. 2).

Results

Table 1 presents information relating to each horse's age, number of race starts, and grading of their micro- and macroscopic appearances. Definitions for each grade of microdamage are provided in Table 2. For the purposes of comparison we have defined the 'younger' age group as those horses 5 years and under. This distinction conveniently corresponded to a substantial increase in number of race starts, such that the younger animals had ≤12 race starts in comparison with their older counterparts with ≥21 race starts.

Macroscopic examination

Macroscopic appearance of the parasagittal groove

Linear fissures in the parasagittal grooves were generally mild, with the majority of condyles in both age groups displaying at most faint grooves in intact cartilage (grade ≤1, see Fig. 3A,B). Occasionally, linear fissures involved localised partial thickness splits in the cartilage (grade = 2, see Fig. 3D).

Macroscopic appearance of the mid-condylar region

Evidence of POD in the mid-condylar region was absent (grade = 0) in both condyles of almost all younger animals, whereas the older animals all had visible discoloration (grade = 1) that was sometimes accompanied by limited cartilage disruption (grade = 2, see Fig. 3C). Three joints exhibited notable macroscopic appearance in the mid-condylar region. The first, a younger animal, had a distinct lesion that was more opaque and slightly sunken in appearance relative to the surrounding cartilage (see arrowhead in Fig. 3A). Another young animal exhibited unusually

Table 2 . Definitions for each grade of microdamage in the two regions of interest.

Mid-condylar	
Mild	Few visible cracks. Little or no disruption of overlying cartilage.
Moderate	Some bone microdamage: either a network of microcracks, showing early signs of lateral fracture formation, or shallow and highly localised subchondral collapse. Little or no disruption of overlying cartilage.
Severe	Extensive subchondral micro-cracking, involving one or more of bone comminution, lateral fracture, and/or subchondral collapse. Typically substantial disruption of overlying cartilage, often accompanied by reparative tissue at the articular surface.
Parasagittal groove	
Mild	Occasional cracks in the calcified cartilage, predominately slopping towards the sagittal ridge, sometimes associated with clusters of much smaller subchondral bone cracks.
Moderate	Frequent cracks in both the calcified cartilage and subchondral bone, typically exhibiting an oblique/counter-oblique morphology. Limited disruption of the deep zone hyaline cartilage may be present.
Severe	Extensive cracking of the calcified cartilage and subchondral bone with the formation of large hyaline cartilage lesions in association with the hard tissue microdamage.

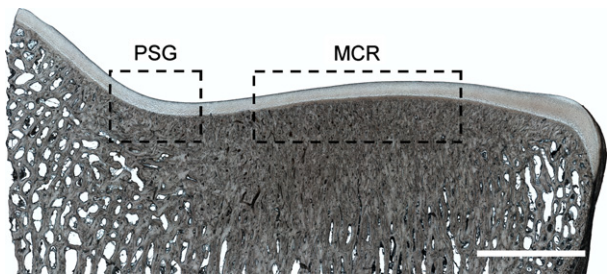

Fig. 2 An example section from the medial condyle of Horse 8, with boxed regions indicating the locations of this studies regions of interest: the parasagittal groove (PSG) and mid-condylar region (MCR). High subchondral bone density can be seen beneath the mid-condylar region and extending to a lesser degree into the parasagittal groove. Scale bar: 5 mm.

(for its age group) clear discoloration beneath intact cartilage in one condyle (see arrow in Fig. 3B). One older animal, while lacking clear signs of discoloration, had a large area of the mid-condylar region where the joint surface was noticeable sunken, i.e. with collapse of the articular surface (Fig. 3D, tentative grade = 3).

General macroscopic appearance

The condition of the MC3 more generally (i.e. not restricted to the two regions of interest) was also graded, specifically for wear lines and cartilage loss associated with the transverse ridge. Wear lines were present in approximately half of the younger animals and were typically very subtle, often being only faintly visible under oblique illumination (grade = 1). In the older animals, wear lines were always present and were generally more distinct than in the younger animals (most clearly visible in Fig. 3C), often being some combination of more numerous, wider and deeper (but still partial thickness, grade = 1). At the transverse ridge (the slight discontinuity in the radius of curvature between the palmar and dorsal aspects of the condyle), cartilage loss, when present, was limited to subtle, highly localised partial thickness disruptions in the younger animals (grade $\leq$1). All older animals had some degree of cartilage disruption at the transverse ridge, typically more extensive than seen in the younger animals (Fig. 3C,D), and in some cases including full thickness ulcerations up to $\approx$10 mm^2 in area, with the previously attached cartilage forming a 'flap' that partially covered the exposed hard tissue (grade = 2).

Microstructural analysis

Microstructural analysis revealed varying degrees of microdamage in the calcified cartilage and subchondral bone in both the parasagittal groove and mid-condylar region, often occurring beneath intact hyaline cartilage. The area between these two regions of interest was generally devoid of visible damage. A common feature of all samples was high subchondral bone density, particularly in the mid-condylar region, where there was a near-complete absence of trabecular spaces to a depth of several millimetres subjacent to the cartilage (see Fig. 2).

Microstructural damage associated with the parasagittal groove

Microdamage was present in both parasagittal grooves of all but one animal (Horse 3). In the younger horses this damage was typically categorised as mild, or less frequently as moderate, and consisted of occasional mid-sized cracks through the calcified cartilage (Fig. 4), sometimes terminating in lesions in the deep zone hyaline cartilage (see arrows in Fig. 4B,C). This damage was often accompanied by clusters of much smaller cracks in the subjacent bone (see boxed region in Fig. 4B). Further, there was some evidence that intense microcracking in the calcified cartilage was linked with a localised area of lesser calcified cartilage thickness, giving the appearance of a recess in the tidemark (see arrows in Fig. 5C).

In the older horses the microdamge was frequently categorised as moderate or severe. Compared with the younger horses, a greater intensity of subchondral bone

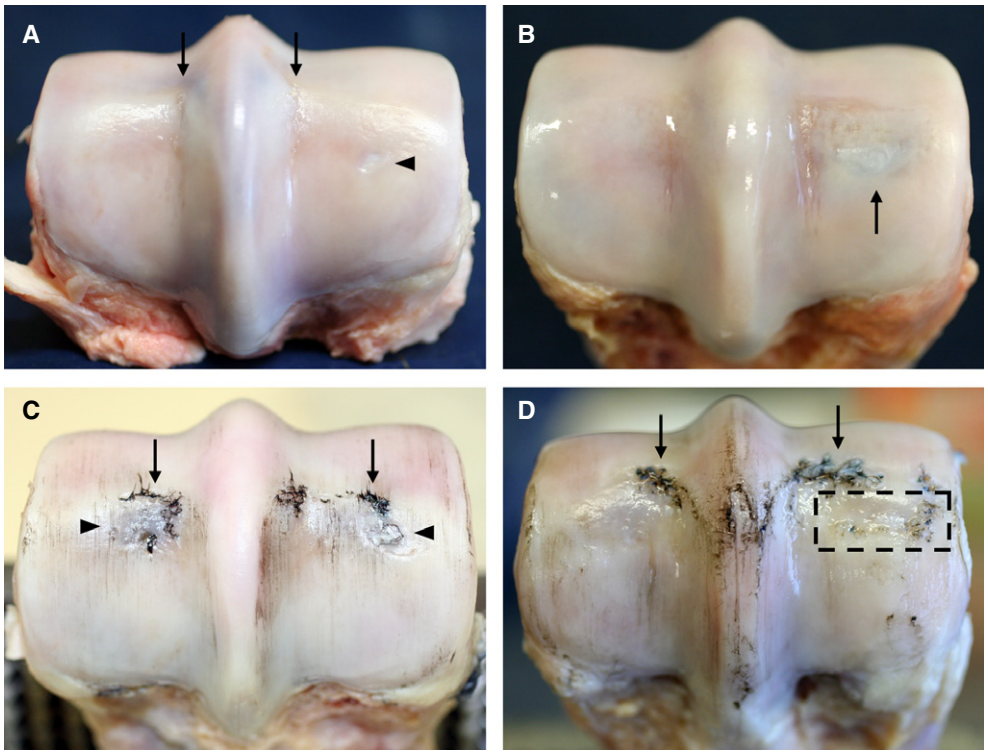

Fig. 3 Macroscopic images of the distal end of the MC3 from younger (A,B) and older (C,D) animals. Lateral is to the left in all images. (A) Horse 5 showing an intact cartilage surface except for very slight linear fissures in the parasagittal grooves (see arrows). Note the small oval-shaped area of opaque white cartilage visible in the centre of the medial condyle region (see arrowhead). (B) Horse 4 with a slightly darkened region beneath undisrupted cartilage (see arrow). (C) Horse 14 showing minor wear lines, significant disruption at the transverse ridges (see arrows), and some darkening beneath the cartilage in the central condylar regions (see arrowheads), especially laterally. (D) Horse 13 showing a further example of cartilage disruption at the transverse ridge (see arrows). There is an area of the mid-condylar region where the joint surface is noticeably sunken in i.e. collapse of the articular surface (boxed region).

damage was observed and the cracks in the calcified cartilage were generally larger, more numerous, and more frequently penetrated into the hyaline cartilage (Fig. 5). It should be noted that the cracks in both the subchondral bone and the calcified cartilage of the parasagittal groove were aligned at approximately 45° to the local articular surface, and at higher crack densities had an oblique/counter-oblique intersecting morphology, with cracks of varying sizes forming fractal arrays (see especially enlarged Fig. 5C).

As also seen in the younger animals, where the cracks advanced across the most distal tidemark they were often associated with lesions in the hyaline cartilage. In the older animals these lesions were generally more pronounced, with some extending almost to the articular surface (Fig. 5A,B). The hyaline cartilage matrix immediately adjacent to these lesions was clearly modified in terms of cell clustering, acellularity and matrix alignment, as indicated by the lines of chondrocyte continuity (Fig. 5C). As in the younger animals, focal areas of lesser calcified cartilage thickness could occasionally be found in association with intense microdamage (Fig. 5C).

Microstructural damage associated with the mid-condylar region

Of the 10 younger animals, seven exhibited no microscopic evidence of damage in the mid-condylar region. There was no obvious microcracking of the calcified cartilage or subchondral bone, no articular surface disruption, and the hyaline cartilage matrix appeared normal (Fig. 6). The remaining three younger animals (Horses 4, 5, 7) displayed notable lesions, which were categorised as exhibiting moderate levels of microdamage. In the older animals, lesions were both more frequent and generally more extensive, with five of the six animals displaying moderate to severe levels of microdamage (Table 1). In both age groups two distinct types of lesion were identified.

The first type of lesion, in the younger animals, involved a shallow, highly localised collapse of the subchondral bone, with the overlying hyaline cartilage folding into the resultant void in the subchondral plate (Fig. 7). Additionally, a clearly discernible layer of 'darker' tissue had formed at the articular surface (see Fig. 7) that corresponds to the opaque cartilage observed macroscopically (Fig. 3A).

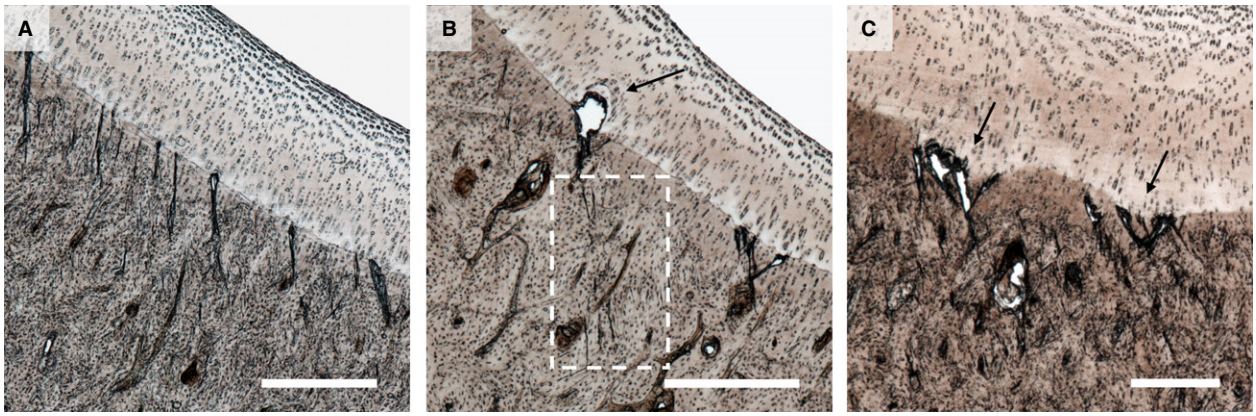

Fig. 4 Examples of microdamage in the parasagittal groove of younger horses. (A) Mild microdamage in Horse 4 showing a cluster of obliquely aligned calcified cartilage microcracks beneath intact hyaline cartilage. Scale bar: 500 μm. (B) Moderate microdamage in Horse 5 showing microcracks associated with lesion formation in the overlying hyaline cartilage (see arrow). Note also the more subtle but similarly aligned cracks in the subchondral bone (see boxed region). Scale bar: 500 μm. (C) Moderate microdamage in Horse 6 showing two distinct recesses in the calcified cartilage closely associated with microdamage (see arrows), as well as small lesions (voids) at the same locations. Scale bar: 300 μm.

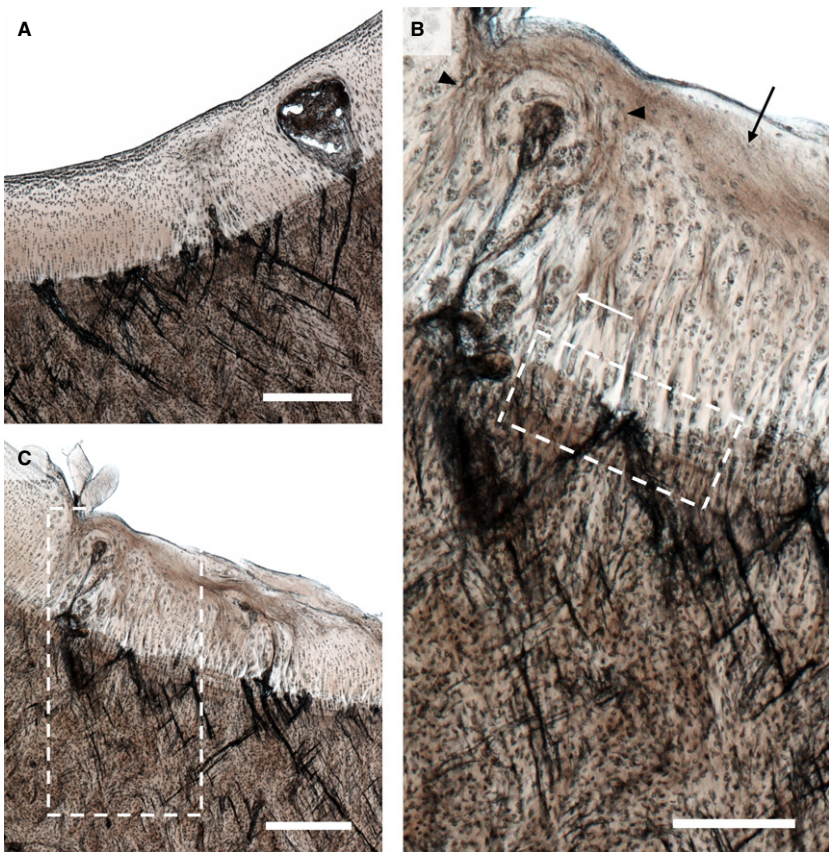

Fig. 5 Severe lesions in the hyaline cartilage and extensive microdamage in (A) the lateral and (B) the medial parasagittal groove of Horse 13. Note the high density of microcracks aligned in a cross-hatch configuration, with many large cracks extending across the calcified cartilage layer. Scale bars: 500 μm. (C) Enlarged image of the boxed region in (B). A number of changes can be seen in the hyaline cartilage including cell clustering (white arrow), regions of acellularity (black arrow), and regions of altered chondrocyte alignment suggestive of matrix remodelling (see black arrow heads). Cracks of various sizes can be seen in the calcified cartilage and subchondral bone. Scale bar: 250 μm.

This 'neo-tissue' was readily distinguishable from, yet structurally integrated with, the underlying hyaline cartilage. Higher magnification imaging (Fig. 7B) indicated that it was highly fibrous in nature and devoid of chondrocytes. No such neo-tissue was seen in the other younger animals.

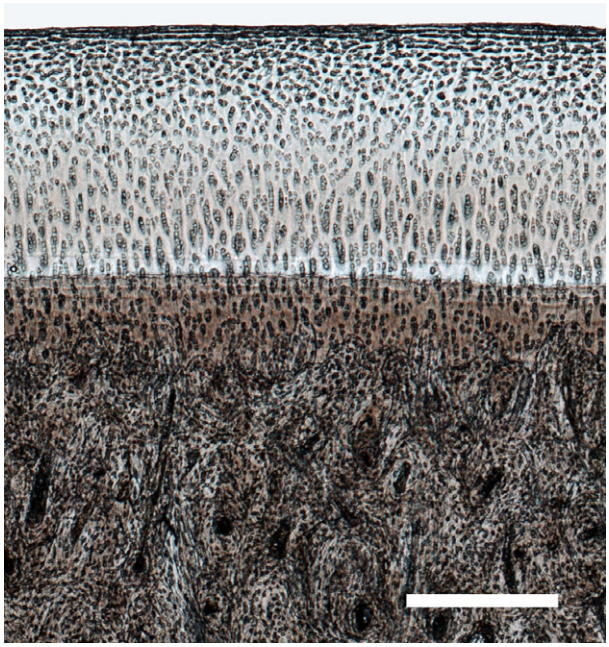

Fig. 6 Higher magnification image from the boxed mid-condylar region in Fig. 3, showing undamaged hyaline and calcified cartilage, and subchondral bone in the midcondylar region for the young Horse 8. Scale bar: 400 μm.

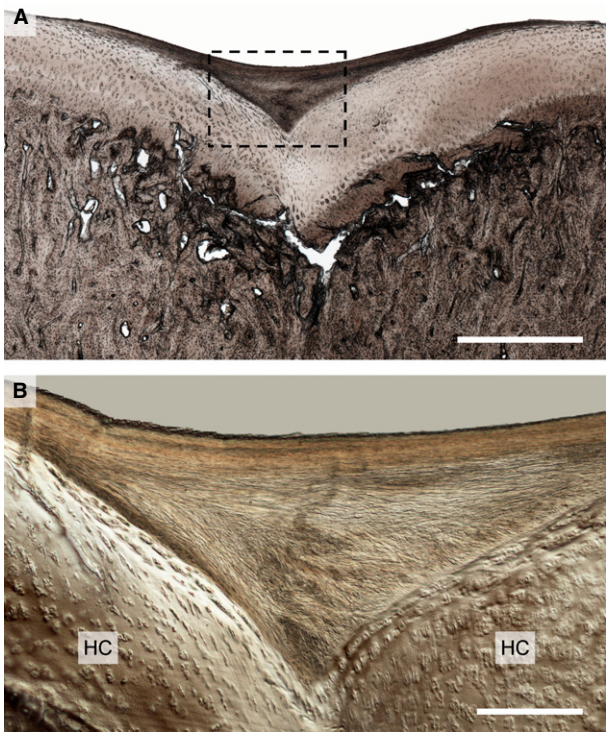

Fig. 7 Moderate damage in the mid-condylar region of Horse 5 showing the example of the first observed lesion type in a younger animal. (A) Low magnification view showing subchondral bone collapse and cartilage infolding in the mid-condylar region. Note the contrasting layer of 'neo-tissue' at the articular surface. Scale bar: 1 mm. (B) Higher magnification DIC image of the boxed region in (B). The neo-tissue that has formed is more fibrous in appearance and devoid of chondrocytes, thus being easily distinguished from the hyaline cartilage (HC) beneath, with which it is structurally integrated. Scale bar: 250 μm.

A similar type of lesion was found in the older animals (Fig. 8), in this case categorised as severe. Externally, the articular surface appeared largely intact, and as such it was difficult to detect macroscopically (boxed region in Fig. 3). Severe subchondral bone collapse was visible (left of Fig. 8A) with the resultant void having been partially filled by both cartilage infolding and loose cartilage and bone fragments. Another region of subchondral subsidence was evident, this time appearing more stable (right of Fig. 8A). The subchondral bone adjacent to these sites showed considerable evidence of microdamage accumulation, with the oblique/counter-oblique microcracks appearing to have progressed such that the bone in the central-most region has a comminuted appearance (shown enlarged in Fig. 8B). Both sites of subsidence were associated with an abnormal thickening of the overlying hyaline cartilage, with regions of contrasting neo-tissue having formed at the articular surface. This tissue varied somewhat in its microstructure: in some regions it had a fibrous texture with a distinct boundary separating it from the hyaline cartilage, similar to that seen in the younger animals (see Fig. 7B); in other regions the fibrous structure appeared less organised and blended more gradually into the underlying hyaline cartilage (see Fig. 8C). Examples of similar neo-tissue were found in three of the six older animals.

The second of the two mid-condylar lesions noted in the three younger animals exhibited obvious subchondral damage spread across a large area (Fig. 9) and corresponded to macroscopically observed discoloration (as in Fig. 3B). The subchondral bone microcracks in this region are chaotic, exhibiting less clearly the oblique/counter-oblique morphology noted earlier. Further, microcrack coalescence has resulted in the formation of a larger laterally spreading fracture in the subchondral plate (see region arrows in Fig. 9).

An example of a severe lesion of the same type from an older animal (Fig. 10) shows more advanced crack coalescence, leading to a much larger lateral fracture. One end of this large fracture breaches the distal-most tidemark and is associated with a distortion of the hyaline cartilage matrix (see enlarged view in Fig. 10B). At the lesion periphery the typical oblique/counter-oblique crack morphology is present (see arrowed site in Fig. 10B), while directly subjacent to the lateral fracture the bone has a comminuted appearance (see enlarged image in Fig. 10C). Examples of this type of mid-condylar lesion seen in both the younger and older animals were always associated with a macroscopically visible discoloration beneath the articular cartilage. Additionally, this lesion was associated with the formation of fibrous

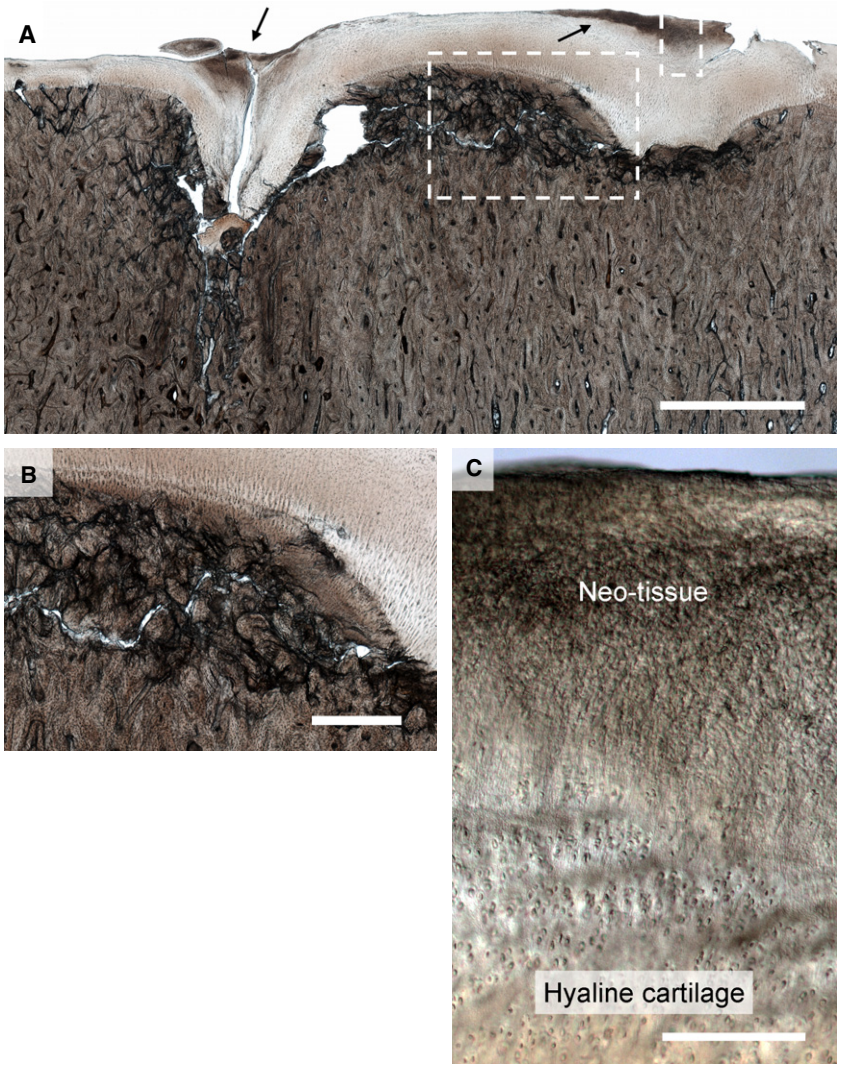

Fig. 8 Severe damage in the mid-condylar region of Horse 13. (A) Low magnification image. Subchondral bone collapse can be seen on the left with cartilage infolding. On the extreme right of the image there is evidence of what appears to be earlier subchondral collapse that may have stabilised. In both cases there is a greater amount of cartilage present than would be expected in a healthy region of the joint, with darker regions of neo-tissue at the articular surface (see arrows). The subchondral bone between the two collapsed regions has a comminuted appearance. Scale bar: 2.5 mm. (B) Enlarged view of left hand boxed region in (A) showing severe damage in the subchondral bone, which as a result has a comminuted appearance. Scale bar: 750 μm. Enlarged view of right hand boxed region in (A) showing the fibrous neo-tissue blending into the underlying hyaline cartilage. Scale bar: 200 μm.

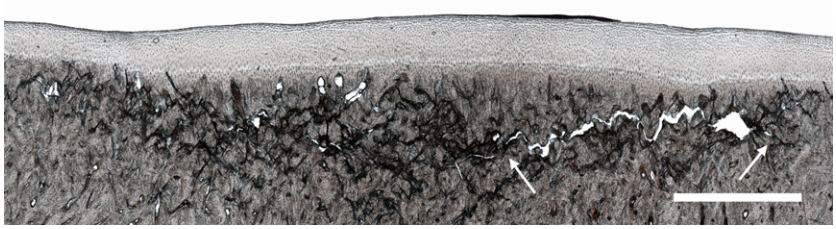

Fig. 9 Moderate microdamage accumulation in the subchondral bone beneath intact hyaline cartilage in Horse 4. Note coalescence of smaller cracks into a larger lateral fracture whose span is indicated by the white arrows. Scale bar: 2 mm.

neo-tissue at the articular surface (Fig. 10A) with a very similar appearance to that observed in the younger animal (Fig. 7).

Finally, a clear example of a tidemark recess was found in the mid-condylar region (Fig. 11), similar to that seen in the parasagittal groove.

Discussion

Microdamage accumulation, due to repetitive overloading, is a common problem affecting the palmar aspect of the distal end of the MC3 of Thoroughbred athletes (Pool, 1996; Radtke et al., 2003; Muir et al., 2008). In this study a range of microdamage severity was observed in two clinically important sites, the medial and lateral parasagittal grooves and mid-condylar regions, with a general trend of increasing levels of damage with increasing animal age. This has enabled us to investigate the general morphological progression of damage arising from repetitive overloading in the joint of a large athletic animal.

Overall, in both the parasagittal groove and mid-condylar region, older animals had a higher intensity of microcrack-

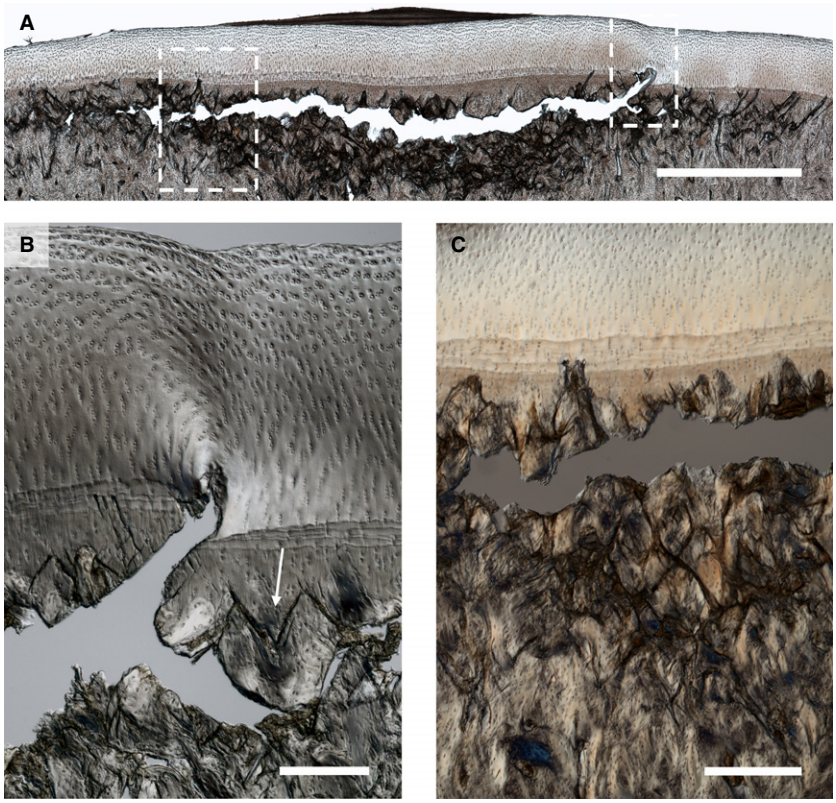

Fig. 10 Severe subchondral bone failure in the mid-condylar region of Horse 14. (A) Low magnification image. The bone at the centre of the lesion has a comminuted appearance, with less intense damage accumulation at the periphery. A large subchondral fracture can be seen subjacent to the calcified cartilage region, which at the right of the image penetrates through to the deep articular cartilage (see right hand boxed region). The articular surface is intact, although a layer of fibrous neo-tissue has formed above the centre of the lesion. Scale bar: 2 mm. (B) Enlarged view of right hand boxed region in (A) showing failure of the calcified cartilage and penetration of the large crack into the hyaline cartilage. Note also the oblique/counter-oblique cracking of the subchondral bone (see arrow). Scale bar: 250 μm. (C) Image showing enlarged view of comminuted subchondral bone from same lesion site as indicated by the left hand boxed region in (A). Scale bar: 200 μm.

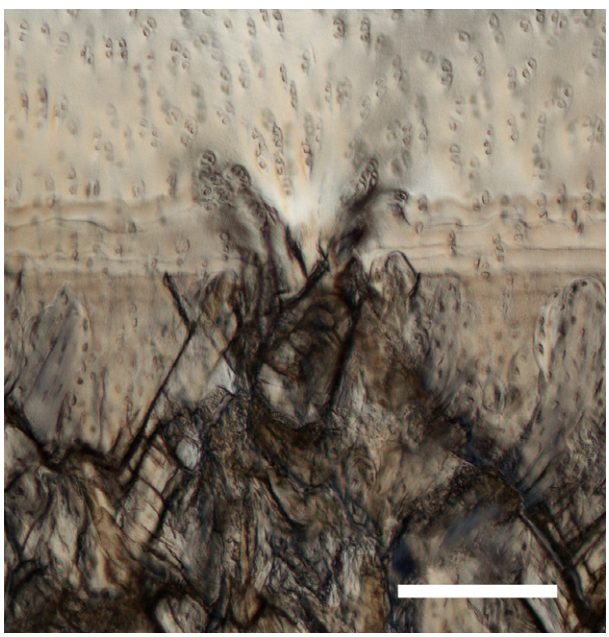

Fig. 11 A calcified cartilage recess associated with microcracking in the mid-condylar region Horse 14. Scale bar: 200 μm.

ing (in terms of both crack number and size) in the calcified cartilage and subchondral bone compared with younger animals (cf. Figs 4, 5, 7–10). Especially noticeable at high crack densities were fractal arrays of microcracks with a distinct oblique/counter-oblique crack morphology characteristic of failure occurring along the planes of maximum shear stress orientated at ~45° to the principal loading axis. In a congruent joint, this axis would be approximately normal to the articular surface. It appears that accumulation of these oblique/counter-oblique microcracks at some stage leads to the comminuted appearance of the subchondral bone seen in the severe mid-condylar lesions in the older animals (see Figs 8B and 10C).

All of the 10 younger horses had microdamage in the parasagittal groove, and only three had detectable damage in the mid-condylar region (see Table 1). By contrast, damage was detected in both the parasagittal groove and mid-condylar region in all but one of the six older horses. This suggests that microdamage development in the parasagittal groove precedes that in the mid-condylar region. Additionally, the mode or order of tissue structural failure was different from that in the mid-condylar region. In the younger animals, damage in the calcified cartilage of the parasagittal groove was noticeably more intense than that in the underlying subchondral bone (Fig. 4), suggesting a predisposition to failure initially in the calcified cartilage at this site. Indeed, for all ages of animal, microcracking of the calcified cartilage was typically of greater intensity in the parasagittal groove than in the mid-condylar region, where cracks in the calcified cartilage were relatively infrequent even in the presence of severe subchondral bone damage (see Figs 8B, 9 and 10C). This apparent predisposition to

microdamage of the calcified cartilage in the parasagittal groove is most likely due to differences in loading conditions between the two sites. Further, the pronounced recesses observed in the most distal tidemark of the calcified cartilage in the regions of intense microcracking (see Figs 4C, 5C and 11) could suggest that this microdamage in the hard tissue is interfering with the normal calcification process.

The close association between lesions in the hyaline cartilage and microdamage in both the subchondral bone and calcified cartilage across the entire age spectrum (see Figs 4 and 5) suggests that hard tissue fracture that impinges directly on the deep-zone hyaline cartilage leads to some form of reactive response in the cartilage with subsequent lesion formation. Additionally, these cartilage lesions bear a resemblance, in both morphology and location, to previously described extrusions of mineralised matrix (Boyde et al., 2011). Although our specimen processing and imaging technique did not allow us to determine whether the contents of the lesions in the hyaline cartilage (e.g. Fig. 5A) were mineralised, it is conceivable that they may represent a related form of pathology. Further, where these lesions were associated with voids (see Fig. 4B) they may well have resulted from the artefactual loss of mineralised fragments during preparation, which included a demineralisation procedure.

The microdamage detected in the parasagittal groove correlates well with previous macroscopic observations of subchondral cracking in this region, in terms of both extent and gross morphology (Riggs et al., 1999; Radtke et al., 2003; Muir et al., 2008). Further, the hard tissue and hyaline cartilage lesions described in the present study appear to correspond to the parasagittal linear fissures reported elsewhere (Riggs et al., 1999; Barr et al., 2009). The observed increase in microcrack density with increasing animal age (and number of race starts) supports the suggestion that these lesions develop via a process of fatigue (Riggs et al., 1999; Riggs, 2002; Radtke et al., 2003; Pinchbeck et al., 2013a) and may progress eventually to the catastrophic condylar fractures documented at this site (Ellis, 1994; Zekas et al., 1999).

The microdamage in the mid-condylar region, while having many morphological features in common with those observed in the parasagittal groove, differed considerably in the type and severity of lesion developed. The mid-condylar region of younger horses typically lacked any visible sign of damage (Fig. 6), with the very dense subchondral bone being the only evidence of high *in vivo* loading (Fig. 2). The few moderate lesions that were present in the younger animals appeared to correspond to similar but more advanced lesions in the older animals (cf. Figs 7–10). In these older animals the mid-condylar lesions were frequently of greater severity and more extensive than those in the parasagittal groove (cf. Figs 5 and 8), which suggests that although damage in the parasagittal groove generally develops at an earlier stage, lesions in the mid-condylar region often progress to a more advanced state.

Although high levels of subchondral bone damage in the mid-condylar region often occurred with no visible damage to the overlying articular surface (see Figs 9 and 10), eventually the hard tissue damage appears to escalate such that the deep hyaline cartilage is compromised. For example, the right hand extremity of the main coalesced crack in Fig. 10A has penetrated the calcified cartilage and hyaline cartilage to create what appears to be an incipient cartilage lesion (enlarged in Fig. 10B). Severe examples are shown in Fig. 8A, where subchondral bone collapse has caused the hyaline cartilage to fold inwards into a void in the subchondral plate. The fibrous 'neo-tissue' at the articular surface at these sites of cartilage infolding (see Fig. 7; arrowed sites in Fig. 8A,C) appears to be reparative in nature, and would help to maintain congruency in the joint following the collapse of the subjacent subchondral bone. Our microstructural evidence indicates that this reparative tissue differs structurally, and probably materially, from the original hyaline cartilage (see Figs 7B and 8C), but its exact nature remains unclear.

The changes observed in the mid-condylar region were characteristic of palmar osteochondral disease (Pool, 1996; Norrdin et al., 1998; Barr et al., 2009) and consistent with reports of similar lesions involving subchondral bone loss with associated cartilage damage (Riggs et al., 1999) and infolding of hyaline cartilage following subchondral collapse (Norrdin et al., 1998; Muir et al., 2008). The high level of hard tissue microdamage that was often found beneath regions of intact hyaline cartilage (Figs 8–10) supports the idea that substantial disruption to the subchondral bone precedes cartilage degeneration in the development of these lesions (Riggs et al., 1999), and also provides further evidence for the development of these lesions by a process of fatigue (Pool, 1996). Further, our study provides additional evidence that the mid-condylar lesions are anatomically independent of those in the parasagittal groove (Pool & Meagher, 1990; Pool, 1996), being spatially and often temporally distinct. This is an important point when considering the pathogenesis of condylar fractures.

It is important to note that much of the subchondral damage observed in this study was either undetectable or only subtly apparent from external examination of the joint surface. Outwardly intact hyaline cartilage often masked considerable hard tissue microdamage. In the parasagittal groove, mild microdamage (similar to Fig. 4A) was usually present despite no external evidence (linear fissures grade = 0), and even severe microdamage (including large cartilage lesions as in Fig. 5) was only reflected externally by a faintly visible groove (grade = 1 or 2). In the mid-condylar region, moderate levels of microdamage (similar to that in Fig. 9) often corresponded to only subtle discoloration when viewed externally (POD grade = 1), with severe microdamage (e.g. Figs 8 and 10) typically corresponding to

slightly darker discoloration accompanied by limited disruption of the cartilage surface (grade = 2). This discoloration in the mid-condylar region in association with moderate to severe levels of microdamage seems likely to be the result of haemorrhage within the subchondral bone. The formation of fibrous neo-tissue in some condyles further concealed the full extent of injury by partially compensating for collapse of the hyaline cartilage/subchondral bone. Additionally, the presence of high levels of microdamage beneath a layer of neo-tissue in Horses 5 and 13 (Figs 7 and 8, respectively) without apparent discoloration (Fig. 2A,D) suggests that this neo-tissue may also obscure discoloration of the subchondral bone. The discoloration may be obscured either by the resultant increase in total soft-tissue thickness and/or by the greater opacity of neo-tissue in comparison with hyaline cartilage.

The deleterious effects of repetitive loading appear to persist even after substantial rest periods. Both Horses 9 and 15, despite being euthanised 163 days and 90 days after their last day of training, respectively, showed substantial microdamage-related cartilage changes and, to a lesser extent, retained evidence of hard tissue microdamage, predominantly in the calcified cartilage. This suggests that the accumulation of microdamage due to the fatigue loading experienced during racing and training may result in continued joint health problems in later life.

Horse 16, despite being 8 years of age and having the greatest number of race starts (57), showed relatively mild damage in both the parasagittal groove and mid-condylar region, indicating that a long racing career need not inevitably lead to severe damage in these regions.

To conclude, this study has provided a detailed, micro-level insight into the progression of repetitive overload arthrosis in the palmar aspect of the third metacarpal of the equine athlete. The study has identified extensive levels of hard tissue microdamage concealed beneath the outwardly intact hyaline cartilage, and has revealed the progression from initial microcrack formation through to severe subchondral bone collapse and lesion formation in the hyaline cartilage.

Acknowledgements

The authors would like to thank the Equine Trust (NZ) for their generous financial support.

References

Barr ED, Pinchbeck GL, Clegg PD, et al. (2009) Post mortem evaluation of palmar osteochondral disease (traumatic osteochondrosis) of the metacarpo/metatarsophalangeal joint in thoroughbred racehorses. *Equine Vet J* **41**, 366–371.

Biewener AA (1993) Safety factors in bone strength. *Calcif Tissue Int* **53**, S68–S74.

Biewener AA, Thomason J, Goodship A, et al. (1983) Bones stress in the horse forelimb during locomotion at different gaits: a comparison of two experimental methods. *J Biomech* **16**, 565–576.

Boyde A, Riggs CM, Bushby AJ, et al. (2011) Cartilage damage involving extrusion of mineralisable matrix from the articular calcified cartilage and subchondral bone. *Eur Cells Mater*, **21**, 470–478.; discussion 478.

Burr DB, Radin EL (2003) Microfractures and microcracks in subchondral bone: are they relevant to osteoarthrosis? *Rheum Dis Clin North Am* **29**, 675–685.

Ellis DR (1994) Some observations on condylar fractures of the third metacarpus and third metatarsus in young thoroughbreds. *Equine Vet J* **26**, 178–183.

Firth EC, Rogers CW, Doube M, et al. (2005) Musculoskeletal responses of 2-year-old Thoroughbred horses to early training. 6. Bone parameters in the third metacarpal and third metatarsal bones. *N Z Vet J* **53**, 101–112.

Frost HM (1994) Perspectives: a biomechanical model of the pathogenesis of arthroses. *Anat Rec* **240**, 19–31.

Harrison SM, Whitton RC, Kawcak CE, et al. (2010) Relationship between muscle forces, joint loading and utilization of elastic strain energy in equine locomotion. *J Exp Biol* **213**, 3998–4009.

Johnson BJ, Stover SM, Daft BM, et al. (1994) Causes of death in racehorses over a 2 year period. *Equine Vet J* **26**, 327–330.

Martin RB, Stover SM, Gibson VA, et al. (1996) *In vitro* fatigue behavior of the equine third metacarpus: remodeling and microcrack damage analysis. *J Orthop Res* **14**, 794–801.

Mori S, Harruff R, Burr DB (1993) Microcracks in articular calcified cartilage of human femoral heads. *Arch Pathol Lab Med* **117**, 196–198.

Muir P, Peterson AL, Sample SJ, et al. (2008) Exercise-induced metacarpophalangeal joint adaptation in the Thoroughbred racehorse. *J Anat* **213**, 706–717.

Norrdin RW, Stover SM (2006) Subchondral bone failure in overload arthrosis: a scanning electron microscopic study in horses. *J Musculoskelet Neuronal Interact* **6**, 251–257.

Norrdin RW, Kawcak CE, Capwell BA, et al. (1998) Subchondral bone failure in an equine model of overload arthrosis. *Bone* **22**, 133–139.

Pinchbeck GL, Clegg PD, Boyde A, et al. (2013a) Horse-, training- and race-level risk factors for palmar/plantar osteochondral disease in the racing Thoroughbred. *Equine Vet J*, **45**, 582–586.

Pinchbeck GL, Clegg PD, Boyde A, et al. (2013b) Pathological and clinical features associated with palmar/plantar osteochondral disease of the metacarpo/metatarsophalangeal joint in Thoroughbred racehorses. *Equine Vet J*, **45**, 587–592.

Pool RR (1996) Pathologic manifestations of joint disease in the athletic horse. In: *Joint Disease in the Horse*. (eds McIlwraith CW, Trotter GW), pp. 87–104. Philadelphia: W.B. Saunders.

Pool RR, Meagher DM (1990) Pathologic findings and pathogenesis of racetrack injuries. *Vet Clin North Am Equine Pract* **6**, 1–30.

Radin EL, Parker HG, Pugh JW, et al. (1973) Response of joints to impact loading – III. Relationship between trabecular microfractures and cartilage degeneration. *J Biomech*, **6**, 51–54.

Radtke CL, Danova NA, Scollay MC, et al. (2003) Macroscopic changes in the distal ends of the third metacarpal and metatarsal bones of Thoroughbred racehorses with condylar fractures. *Am J Vet Res* **64**, 1110–1116.

Reilly GC, Currey JD, Goodship AE (1997) Exercise of young thoroughbred horses increases impact strength of the third metacarpal bone. *J Orthop Res* **15**, 862–868.

Richardson DW (2003) The metacarpophalangeal joint. In *Diagnosis and Management of Lameness in the Horse*. (eds Ross MW, Dyson SJ), pp. 348–362. St. Louis: Saunders.

Rick MC, O'Brien TR, Pool RR, et al. (1983) Condylar fractures of the third metacarpal bone and third metatarsal bone in 75 horses: radiographic features, treatments, and outcome. *J Am Vet Med Assoc* **183**, 287–296.

Riggs CM (2002) Fractures – a preventable hazard of racing thoroughbreds? *Vet J* **163**, 19–29.

Riggs CM (2006) Osteochondral injury and joint disease in the athletic horse. *Equine Vet Educ* **18**, 100–112.

Riggs CM, Whitehouse GH, Boyde A (1999) Pathology of the distal condyles of the third metacarpal and third metatarsal bones of the horse. *Equine Vet J* **31**, 140–148.

Schaffler MB, Radin EL, Burr DB (1989) Mechanical and morphological effects of strain rate on fatigue of compact bone. *Bone* **10**, 207–214.

Sokoloff L (1993) Microcracks in the calcified layer of articular cartilage. *Arch Pathol Lab Med* **117**, 191–195.

Stashak TS, Hill C (2002) Conformation and movement. In *Adams' Lameness in Horses*. (ed. Stashak TS), pp. 82. Philadelphia: Lippincott Williams & Wilkins.

Stephens PR, Richardson DW, Spencer PA (1988) Slab fractures of the third carpal bone in standardbreds and thoroughbreds: 155 cases (1977–1984). *J Am Vet Med Assoc* **193**, 353–358.

Zekas LJ, Bramlage LR, Embertson RM, et al. (1999) Characterisation of the type and location of fractures of the third metacarpal/metatarsal condyles in 135 horses in central Kentucky (1986–1994). *Equine Vet J* **31**, 304–308.

Zioupos P, Currey JD (1994) The extent of microcracking and the morphology of microcracks in damaged bone. *J Mater Sci* **29**, 978–986.